PERGAMON

International Journal of Solids and Structures 40 (2003) 5139–5156

INTERNATIONAL JOURNAL OF SOLIDS and STRUCTURES

www.elsevier.com/locate/ijsolstr

Nonlinear dynamics and chaos in coupled shape memory oscillators

Luciano G. Machado [a], Marcelo A. Savi [b,*], Pedro Manuel C.L. Pacheco [c]

[a] *Department of Mechanical and Materials Engineering, Instituto Militar de Engenharia, 22.290.270, Rio de Janeiro, RJ, Brazil*
[b] *COPPE—Department of Mechanical Engineering, Universidade Federal do Rio de Janeiro, Cx. Postal 68.503, 21.945.970, Rio de Janeiro, RJ, Brazil*
[c] *CEFET/RJ, Department of Mechanical Engineering, 20.271.110, Rio de Janeiro, RJ, Brazil*

Received 28 August 2002; received in revised form 23 December 2002

Abstract

Shape memory and pseudoelastic effects are thermomechanical phenomena associated with martensitic phase transformations, presented by shape memory alloys. This contribution concerns with the dynamical response of coupled shape memory oscillators. Equations of motion are formulated by assuming a polynomial constitutive model to describe the restitution force of the oscillators and, since they are associated with a five-dimensional system, the analysis is performed by splitting the state space in subspaces. Free and forced vibrations are analyzed showing different kinds of responses. Periodic, quasi-periodic, chaos and hyperchaos are all possible in this system. Numerical investigations show interesting and complex behaviors. Dynamical jumps in free vibration and amplitude variation when temperature characteristics are changed are some examples. This article also shown some characteristics related to chaos–hyperchaos transition.

Keywords: Nonlinear dynamics; Chaos; Hyperchaos; Shape memory alloys

1. Introduction

Inspired by nature, researchers are trying to create systems and structures that can repair themselves, presenting an adaptive behavior according to its environment. Among many options of smart sensors and actuators, employed in this kind of system, one can highlight piezoelectric materials, magnetostrictive materials, electrorheological fluids and shape memory alloys (SMAs) (Rogers, 1995).

SMAs are metallic compounds with the ability to return to a previous shape or dimension, when subjected to an appropriate thermomechanical procedure (Hodgson et al., 1992). Martensitic transformation is

* Corresponding author.
E-mail addresses: savi@ufrj.br (M.A. Savi), calas@cefet-rj.br (P.M.C.L. Pacheco).

0020-7683/$ - see front matter © 2003 Elsevier Ltd. All rights reserved.
doi:10.1016/S0020-7683(03)00260-9

the phenomenon that promotes the shape recovery of these alloys, driving two different effects: pseudo-elasticity and shape memory.

The remarkable properties of SMAs are attracting much technological interest, motivating different applications in several fields of sciences and engineering. They are ideally suited for use as fastener, seals, connectors and clamps (van Humbeeck, 1999). Self-actuating fastener, thermally actuator switches and several bioengineering devices are some examples of these applications (Machado and Savi, 2003; Duerig et al., 1999; Lagoudas et al., 1999). The use of SMAs can help solving many important problems in aerospace technology, in particular those concerning with space savings achieved by self-erectable structures, stabilizing mechanisms, solar batteries, non-explosive release devices and other possibilities (Denoyer et al., 2000). Micromanipulators and robotics actuators have been built employing SMAs properties to mimic the smooth motions of human muscles (Garner et al., 2001; Webb et al., 2000; Rogers, 1995). Moreover, SMAs are being used as actuators for vibration and buckling control of flexible structures. In this particular field, SMAs wires embedded in composite materials have been used to modify mechanical characteristics of slender structures (Birman, 1997; Rogers, 1995). The main drawback of SMAs is their slow rate of change.

Since the martensitic transformation presented by SMAs is intrinsically nonlinear, dynamical response of shape memory systems may present some behavior that cannot be observed in linear systems. Chaotic response is one of these behaviors. Nonlinearity, sensitive dependence on initial conditions and at least three dimensions are some intrinsic characteristics that a dynamical system must have to present a chaotic response. Therefore, chaos is related to long-term unpredictability (Boccaletti et al., 2000; Pecora et al., 1997). Lyapunov exponents evaluate the sensitive dependence on initial conditions estimating the exponential divergence of nearby orbits. These exponents have been used as the most useful dynamical diagnostic tool for chaotic system analysis. The signs of the Lyapunov exponents provide a qualitative picture of the system's dynamics and any system containing at least one positive exponent presents chaotic behavior. The term hyperchaos is employed when the system has more than one positive exponent.

In the past, most of contributions related to chaotic dynamics were concentrated on the evolution analysis of low-dimensional dynamical systems. Nevertheless, several physical systems must be investigated according to a high-dimensional approach, e.g., fluid flows. Recently, the spatiotemporal chaos has attracted so much attention due to its theoretical and practical applications (Awrejcewicz, 1991; Umberger et al., 1989; Lai and Grebogi, 1999; Shibata, 1998).

As an example of application of spatiotemporal chaos one could mention communications, where its use is related to transmission security. A signal can be transmitted with a chaotic pattern in order to avoid identification. Then, synchronization is used to recover the original information (Hu et al., 1997). In medicine, spatiotemporal chaos has been analyzed to investigate the interaction between intelligence and electrical brain activity (Anokhin et al., 1999). In mechanical sciences, smart systems and structures are examples that can present spatiotemporal chaos.

The dynamical response of shape memory systems is addressed in different references (Seelecke, 2002; Gandhi and Chapuis, 2002; Collet et al., 2001; Salichs et al., 2001; Saadat et al., 2002). On the other hand, chaotic response of these systems is reported in Savi and Braga (1993a,b), Savi and Pacheco (2002) and Savi et al. (2002).

This contribution is concerned with coupled shape memory oscillators, investigating spatiotemporal aspects related to its dynamics. The great number of shape memory applications, in several fields of science, motivates the development of this work. A system that is continuous in time and discrete in space is herein explored. This system is modeled by coupled ordinary differential equations. The polynomial constitutive model, proposed by Falk (1980), is used to describe the restitution force of shape memory oscillators. Despite the deceiving simplicity of the model used, the authors agree that this analysis provides a qualitative picture of the response of shape memory systems. The response is evaluated considering free and forced vibration. The prospect of chaotic response is of concern.

2. Equations of motion

In order to model a shape memory system which nonlinear dynamical response represents the qualitative response of shape memory structures, consider a two-degree of freedom oscillator, depicted in Fig. 1. It consists of two masses, m_i $(i = 1, 2)$, connected by SMA elements and linear dampers with coefficient c_i $(i = 1, 2, 3)$. Two forces excite the system harmonically $F_i = \overline{F}_i \sin(\Omega_i t)$ $(i = 1, 2)$.

Shape memory behavior is described by considering a polynomial constitutive model (Falk, 1980). This is a one-dimensional model which represents the shape memory and pseudoelastic effects considering a polynomial free energy that depends on the temperature and on the one-dimensional strain, E. Therefore, the restoring force of the oscillator is given by

$$K = K(u, T) = \bar{a}(T - T_{\mathrm{M}})u - \bar{b}u^3 + \bar{e}u^5. \tag{1}$$

Parameters $\bar{a}$, $\bar{b}$ and $\bar{e}$ are positive constants, while T_{M} is the temperature below which the martensitic phase is stable. Variable u represents the displacement associated with the SMA element. By establishing the equilibrium of the system, dimensionless equations of motion are presented as follows (Savi and Pacheco, 2002):

$$\begin{aligned}
y_0' &= y_1,\\
y_1' &= \delta_1 \sin(\varpi_1 \tau) - (\xi_1 + \xi_2\alpha_{21}\mu)y_1 + \xi_2\alpha_{21}\mu y_3 - [(\theta_1 - 1) + \alpha_{21}^2\mu(\theta_2 - 1)]y_0\\
&\quad + \alpha_{21}^2\mu(\theta_2 - 1)y_2 + \beta_1 y_0^3 - \varepsilon_1 y_0^5 - \beta_2\alpha_{21}^2\mu(y_2 - y_0)^3 + \varepsilon_2\alpha_{21}^2\mu(y_2 - y_0)^5,\\
y_2' &= y_3,\\
y_3' &= \alpha_{21}^2\delta_2 \sin(\varpi_2\tau) + \xi_2\alpha_{21}y_1 - (\xi_2\alpha_{21} + \xi_3\alpha_{21}\alpha_{32})y_3 + \alpha_{21}^2(\theta_2 - 1)y_0\\
&\quad - [\alpha_{21}^2(\theta_2 - 1) + \alpha_{21}^2\alpha_{32}^2(\theta_3 - 1)]y_2 + \beta_2\alpha_{21}^2(y_2 - y_0)^3 - \varepsilon_2\alpha_{21}^2(y_2 - y_0)^5 + \beta_3\alpha_{21}^2\alpha_{32}^2 y_2^3 - \varepsilon_3\alpha_{21}^2\alpha_{32}^2 y_2^5,
\end{aligned} \tag{2}$$

where

$$\omega_1^2 = \frac{a_1 A T_{M_1}}{m_1 L}, \quad \omega_2^2 = \frac{a_2 A T_{M_2}}{m_2 L}, \quad \omega_3^2 = \frac{a_3 A T_{M_3}}{m_2 L}, \tag{3}$$

$$\tau = \omega_1 t, \quad (\,)' = \mathrm{d}(\,)/\mathrm{d}\tau, \quad y_0 = u_1/L, \quad y_1 = u_1'/L, \quad y_2 = u_2/L, \quad y_3 = u_2'/L,$$

$$\varpi_1 = \Omega_1/\omega_1, \quad \varpi_2 = \Omega_2/\omega_1, \quad \theta_i = T_i/T_{M_i} \ \ (i = 1, 2, 3),$$

$$\delta_1 = \frac{\overline{F}_1}{m_1 L\omega_1^2}, \quad \delta_2 = \frac{\overline{F}_2}{m_2 L\omega_2^2},$$

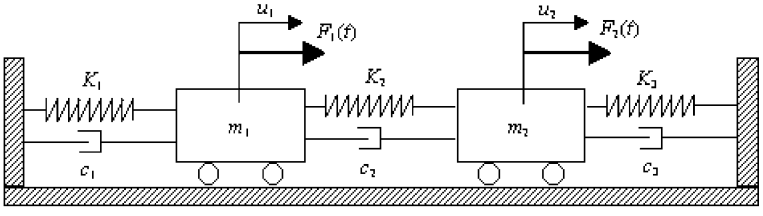

Fig. 1. Two-degree of freedom shape memory oscillator.

$$\xi_1 = \frac{c_1}{m_1\omega_1}, \quad \xi_2 = \frac{c_2}{m_2\omega_2}, \quad \xi_3 = \frac{c_3}{m_2\omega_3},$$

$$\alpha_{21} = \frac{\omega_2}{\omega_1}, \quad \alpha_{32} = \frac{\omega_3}{\omega_2}, \quad \mu = \frac{m_2}{m_1},$$

$$\beta_1 = \frac{b_1 A}{m_1 L\omega_1^2}, \quad \beta_2 = \frac{b_2 A}{m_2 L\omega_2^2}, \quad \beta_3 = \frac{b_3 A}{m_2 L\omega_3^2},$$

$$\varepsilon_1 = \frac{e_1 A}{m_1 L\omega_1^2}, \quad \varepsilon_2 = \frac{e_2 A}{m_2 L\omega_2^2}, \quad \varepsilon_3 = \frac{e_3 A}{m_2 L\omega_3^2}.$$

It is convenient to define the temperature T_A above which only austenitic phase is stable. According to constitutive relations, it is clear that (Savi and Pacheco, 2002)

$$\theta_{Ai} = T_{Ai}/T_{Mi} = 1 + \frac{1}{4}\frac{\beta_i^2}{\varepsilon_i} \quad (i = 1, 2, 3) \tag{4}$$

3. Free vibrations

Numerical simulations are performed by employing a fourth-order Runge–Kutta scheme for which time steps are chosen to be smaller than $\Delta\tau = 2\pi/200$. In all simulations, similar mechanical properties are regarded for all elements of the system. It is assumed a unitary mass and $\varpi_1 = \varpi_2 = 1$, $\xi_1 = \xi_2 = \xi_3 = 0.2$, $\beta_1 = \beta_2 = \beta_3 = 1.3 \times 10^3$ and $\varepsilon_1 = \varepsilon_2 = \varepsilon_3 = 4.7 \times 10^5$. These information lead to the conclusion that $\alpha_{21} = \alpha_{32} = \mu = 1$ and $\theta_{A1} = \theta_{A2} = \theta_{A3} = 1.9$.

Since equations of motion are associated with a five-dimensional system, $\dot{y} = f(y, \tau)$, $y \in R^4$, the visualization of the entire phase space becomes difficult. Therefore, the analysis is performed by splitting the state space into subspaces.

A fixed point, or an equilibrium point, represents an equilibrium solution of a vector field, i.e., a solution that does not change with time. Denoting $\bar{y} \in R^4$ as a fixed point, it is defined as a point that makes the right-hand side of the equations of motion vanish, $f(\bar{y}) = 0$. The shape memory system has different equilibrium points depending on temperature. The analysis of these points, for several temperatures, is performed by considering the intersection of surfaces f with null surface. Fig. 2 presents the intersection of surfaces $f_1(y_0, y_2)$ and $f_3(y_0, y_2)$ with the null surface, projected on the y_0–y_2 plane. Since $\bar{y}_1 = \bar{y}_3 = 0$, these intersections represent equilibrium points. For homogeneous temperatures, where all elements have the same temperature, there are three different sets. Considering lower temperature ($\theta_1 = \theta_2 = \theta_3 = 0.7$), where martensitic phase is stable, the system presents 13 fixed points (Fig. 2a). For intermediate temperatures ($\theta_1 = \theta_2 = \theta_3 = 1.5$), where both martensite and austenite are stable, the system presents 25 equilibrium points (Fig. 2b). For higher temperatures ($\theta_1 = \theta_2 = \theta_3 = 3.5$), where only austenitic phase is stable, there is a single equilibrium point (Fig. 2c). Non-homogeneous temperatures present other different sets as shown in Fig. 2d–h. All of which have a different number of equilibrium points depending on temperatures.

The stability of fixed points is analyzed accessing the spectrum of eigenvalues of the Jacobian matrix. Stable points are associated with eigenvalues with negative real part, while unstable points have positive real part. This way, Fig. 2a–h presents not only the number and position of equilibrium points, but also their stability. Stable equilibrium points are marked with rectangles, while unstable ones are marked with dark circles.

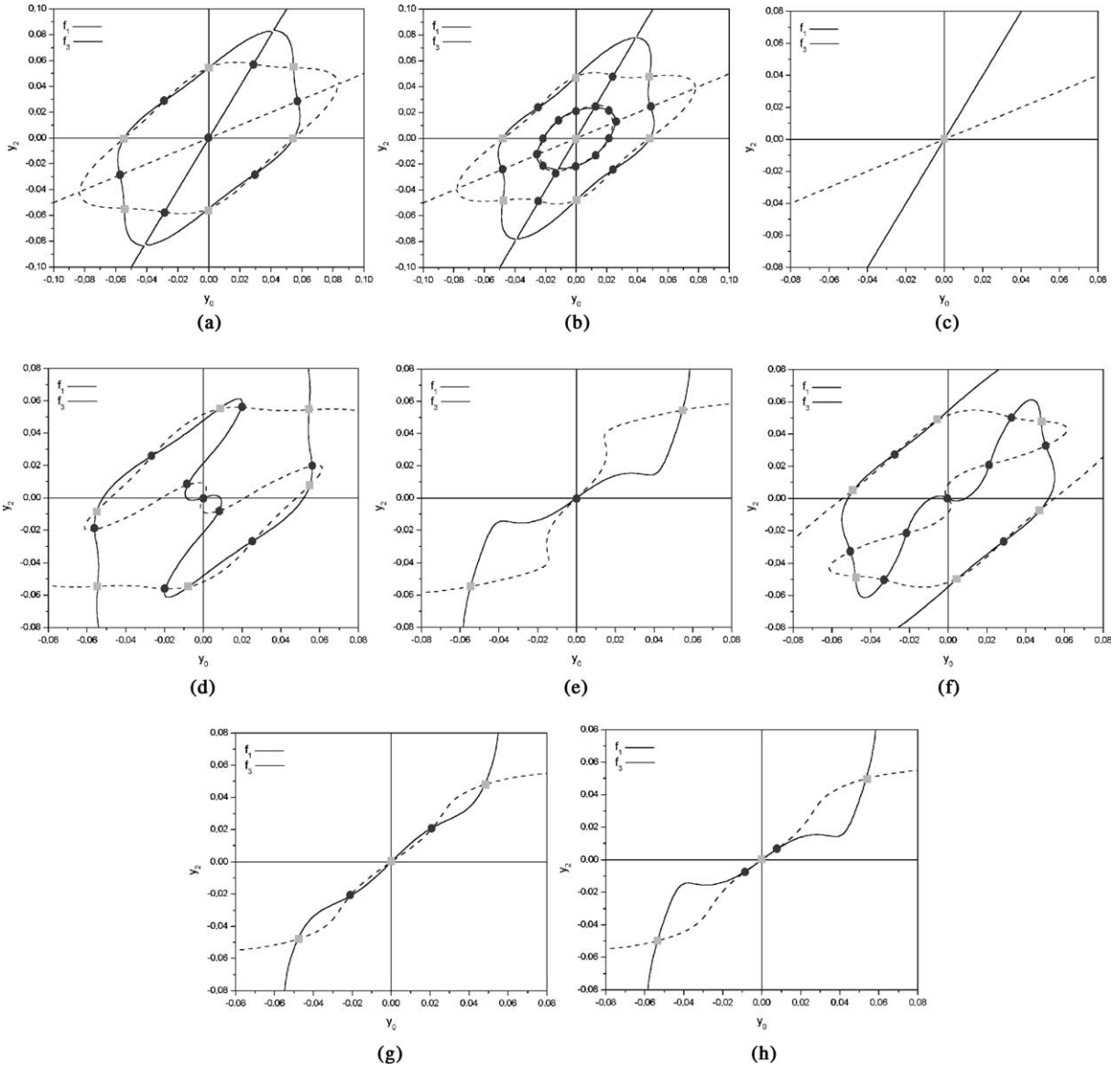

Fig. 2. Identification of equilibrium points, projection of the intersection of surfaces f_1 and f_3 with a null surface: (a) $\theta_1 = \theta_2 = \theta_3 = 0.7$; (b) $\theta_1 = \theta_2 = \theta_3 = 1.5$; (c) $\theta_1 = \theta_2 = \theta_3 = 3.5$; (d) $\theta_1 = 0.7$, $\theta_2 = 1.5$, $\theta_3 = 0.7$; (e) $\theta_1 = 0.7$, $\theta_2 = 3.5$, $\theta_3 = 0.7$; (f) $\theta_1 = 1.5$, $\theta_2 = 0.7$, $\theta_3 = 1,5$; (g) $\theta_1 = 1.5$, $\theta_2 = 3.5$, $\theta_3 = 1.5$; (h) $\theta_1 = 0.7$, $\theta_2 = 3.5$, $\theta_3 = 1.5$.

In order to illustrate the free response of shape memory systems, a situation where $(\theta_1, \theta_2, \theta_3) = (1.5, 0.7, 1.5)$ is considered. For an initial condition $(y_0, y_1, y_2, y_3) = (0.01, 0.0, 0.01, 0.0)$, an interesting transient response occurs when the system tends to converge twice to "false" stable equilibrium points and then, suddenly, jumps to other points. In steady state, the system converges to a "real" stable point. This behavior shows the difficulty to analyze the system response from subspaces related to each mass (Fig. 3). Fig. 4 presents a 3D projection of the phase space, showing the jumps mentioned above.

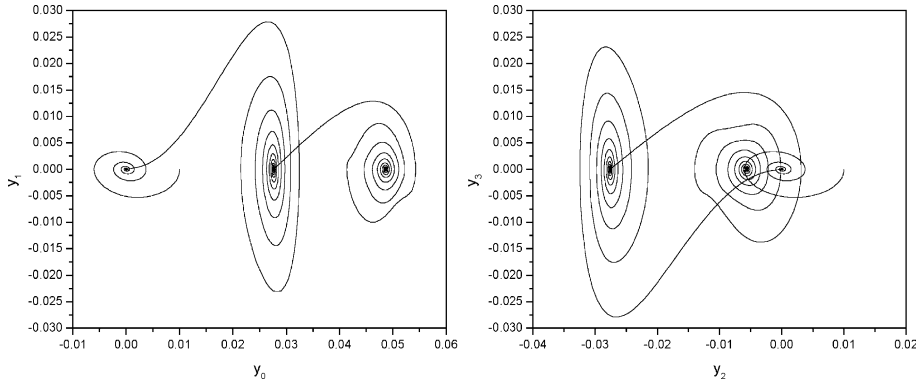

Fig. 3. Free vibration: $(y_0, y_1, y_2, y_3) = (0.01, 0.0, 0.01, 0.0)$ and $(\theta_1, \theta_2, \theta_3) = (1.5, 0.7, 1.5)$.

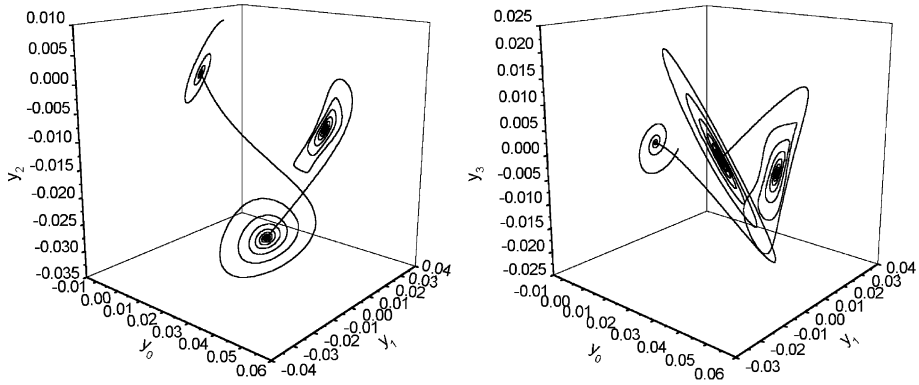

Fig. 4. Free vibration, 3D projection of phase space: $(y_0, y_1, y_2, y_3) = (0.01, 0.0, 0.01, 0.0)$ and $(\theta_1, \theta_2, \theta_3) = (1.5, 0.7, 1.5)$.

4. Forced vibrations

Forced vibration is now focused. The characterization of chaotic, hyperchaotic, quasi-periodic and periodic motion is done by regarding Lyapunov exponents, whose estimation employs the algorithm proposed by Wolf et al. (1985). The analysis is developed by considering different temperature sets for the shape memory elements. At first, consider a situation where $\delta_2 = 0$ and all shape memory elements have a low temperature, i.e., only martensitic phase is stable ($\theta_1 = \theta_2 = \theta_3 = 0.7$). Afterwards, the connection temperature, θ_2 is changed. Fig. 5 shows bifurcation diagrams by varying the parameter δ_1 for three different situations: $(\theta_1, \theta_2, \theta_3) = (0.7, 0.7, 0.7)$, $(\theta_1, \theta_2, \theta_3) = (0.7, 1.5, 0.7)$ and $(\theta_1, \theta_2, \theta_3) = (0.7, 3.5, 0.7)$. These diagrams show how the response of the system is sensitive to temperature changes. For analyzing some particular situations, consider $\delta_1 = 0.06$, $\delta_2 = 0$ and $(\theta_1, \theta_2, \theta_3) = (0.7, 0.7, 0.7)$. Under these conditions, the system presents a chaotic response with Lyapunov exponents $\lambda_i = (+0.19, -0.02, -0.46, -0.86)$ (Fig. 6). By increasing the connection temperature to $\theta_2 = 1.5$, the response becomes hyperchaotic with $\lambda_i = (+0.34, +0.05, -0.55, -1.0)$ (Fig. 7). On the other hand, for $\theta_2 = 3.5$, the system presents a periodic response (Fig. 8).

It should be pointed out that temperature change causes either transition chaos → hyperchaos → periodic response, or vibration amplitude variation. Figs. 9–11 present phase spaces related to the

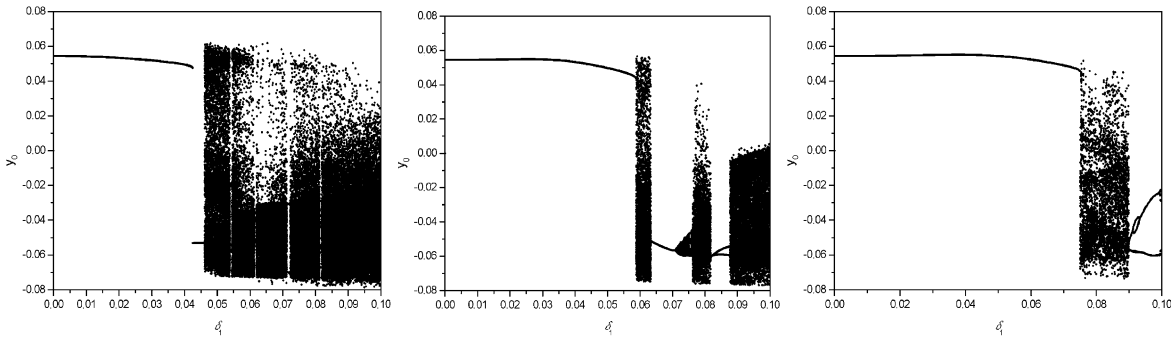

Fig. 5. Bifurcation diagrams for $\delta_2 = 0$: (a) $(\theta_1, \theta_2, \theta_3) = (0.7, 0.7, 0.7)$; (b) $(\theta_1, \theta_2, \theta_3) = (0.7, 1.5, 0.7)$; and (c) $(\theta_1, \theta_2, \theta_3) = (0.7, 3.5, 0.7)$.

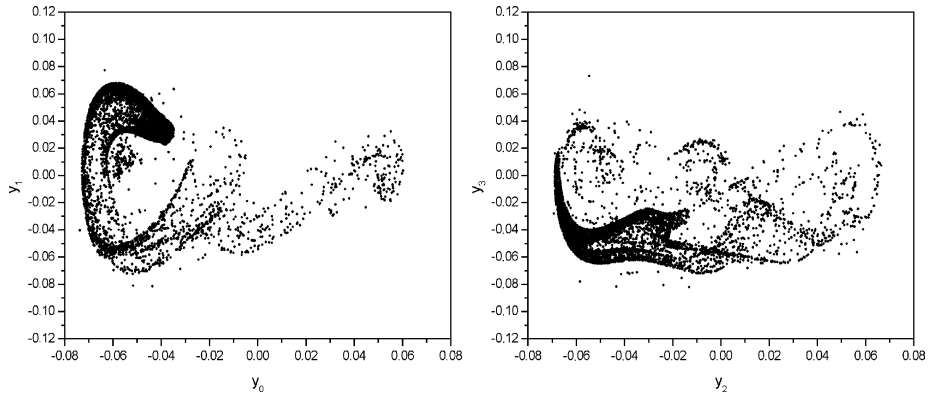

Fig. 6. Chaos: $\delta_1 = 0.06$, $\delta_2 = 0$ and $(\theta_1, \theta_2, \theta_3) = (0.7, 0.7, 0.7)$.

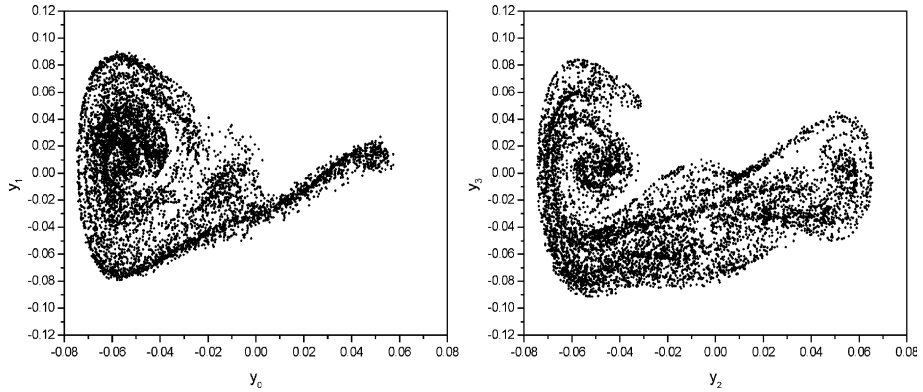

Fig. 7. Hyperchaos: $\delta_1 = 0.06$, $\delta_2 = 0$ and $(\theta_1, \theta_2, \theta_3) = (0.7, 1.5, 0.7)$.

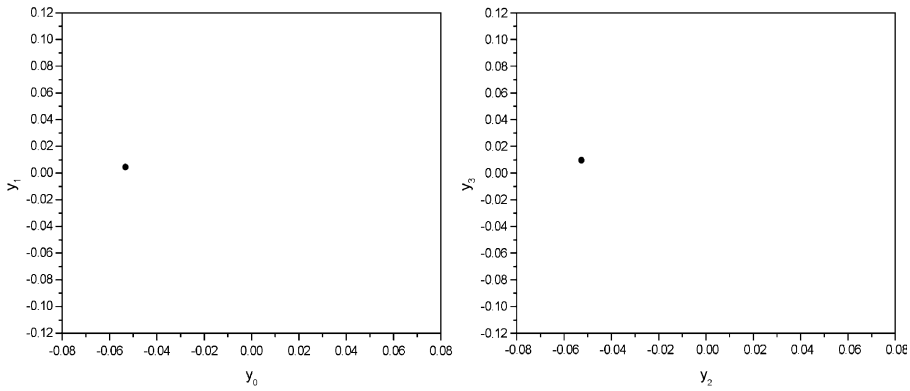

Fig. 8. Periodic response: $\delta_1 = 0.06$, $\delta_2 = 0$ and $(\theta_1, \theta_2, \theta_3) = (0.7, 3.5, 0.7)$.

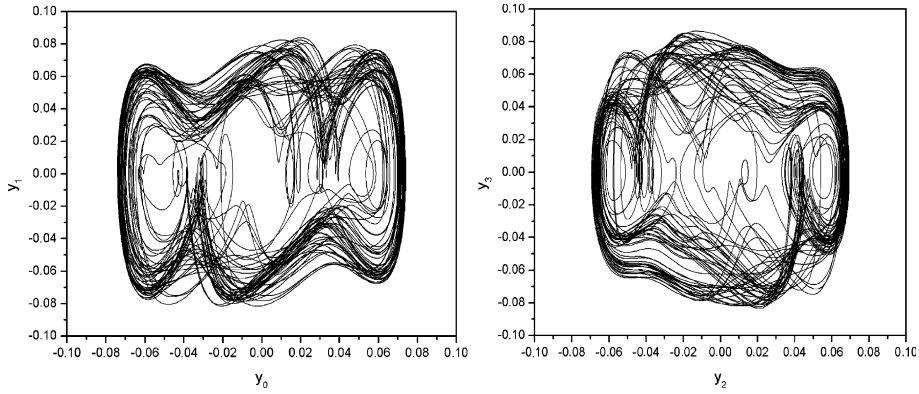

Fig. 9. Chaos: $\delta_1 = 0.06$, $\delta_2 = 0$ and $(\theta_1, \theta_2, \theta_3) = (0.7, 0.7, 0.7)$.

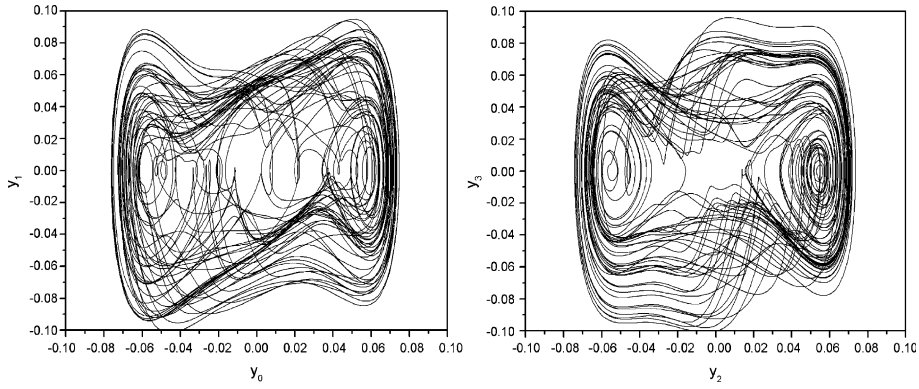

Fig. 10. Hyperchaos: $\delta_1 = 0.06$, $\delta_2 = 0$ and $(\theta_1, \theta_2, \theta_3) = (0.7, 1.5, 0.7)$.

mentioned parameters, showing the amplitude reduction of the responses. Fig. 12 presents a comparison of these three kinds of responses showing their time histories.

A situation where shape memory elements have intermediate temperatures, i.e., both martensitic and austenitic phases are stable ($\theta_1 = \theta_3 = 1.5$), is now considered. Likewise the first example, the connection temperature, θ_2, is changed. Fig. 13 shows bifurcation diagrams by varying δ_1 with $\delta_2 = 0$, for three different situations: $(\theta_1, \theta_2, \theta_3) = (1.5, 0.7, 1.5)$, $(\theta_1, \theta_2, \theta_3) = (1.5, 1.5, 1.5)$ and $(\theta_1, \theta_2, \theta_3) = (1.5, 3.5, 1.5)$. Fig. 14 presents enlargements of Fig. 13a and c. Fig. 14a shows several periodic windows, while Fig. 14b presents a quasi-periodic window.

By observing particular situations, it should be noted that for $\delta_1 = 0.06$, $\delta_2 = 0$ and $(\theta_1, \theta_2, \theta_3) = (1.5, 0.7, 1.5)$, the system presents a periodic response (Fig. 15). By increasing the temperature connection to $\theta_2 = 1.5$, the response becomes chaotic with $\lambda_i = (+0.22, -0.13, -0.30, -0.94)$ (Fig. 16). On the other hand, for $\theta_2 = 3.5$, the system presents a quasi-periodic response with $\lambda_i = (0.00, -0.15, -0.41, -0.66)$ (Fig. 17).

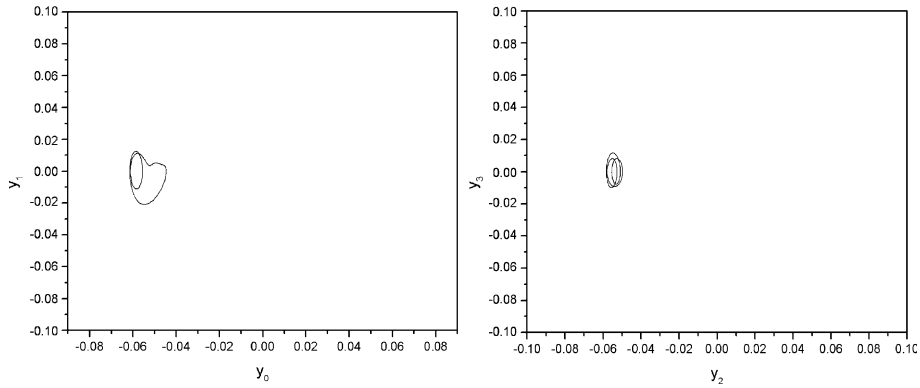

Fig. 11. Periodic response: $\delta_1 = 0.06$, $\delta_2 = 0$ and $(\theta_1, \theta_2, \theta_3) = (0.7, 3.5, 0.7)$.

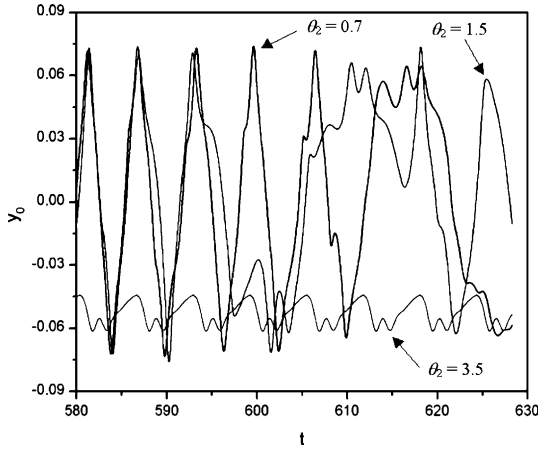

Fig. 12. Time history comparison: $\delta_1 = 0.06$, $\delta_2 = 0$, $(\theta_1, \theta_2, \theta_3) = (0.7, 0.7, 0.7)$, $(\theta_1, \theta_2, \theta_3) = (0.7, 1.5, 0.7)$ and $(\theta_1, \theta_2, \theta_3) = (0.7, 3.5, 0.7)$.

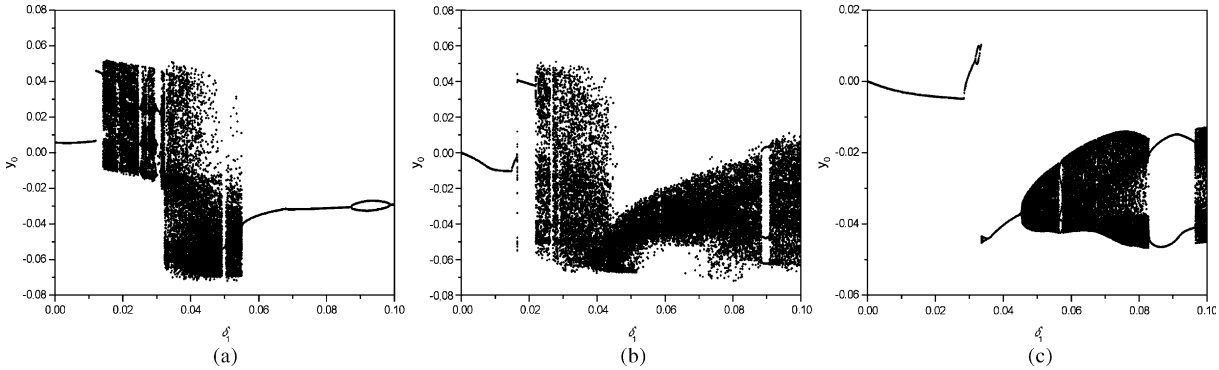

Fig. 13. Bifurcation diagrams for $\delta_2 = 0$: (a) $(\theta_1, \theta_2, \theta_3) = (1.5, 0.7, 1.5)$; (b) $(\theta_1, \theta_2, \theta_3) = (1.5, 1.5, 1.5)$; (c) $(\theta_1, \theta_2, \theta_3) = (1.5, 3.5, 1.5)$.

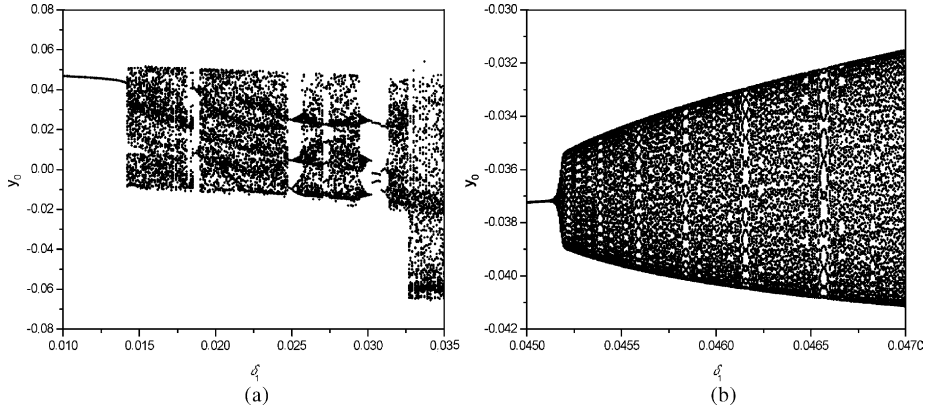

Fig. 14. Enlargements: (a) Fig. 13a, interval: $0.01 \leqslant \delta_1 \leqslant 0.035$; (b) Fig. 13c, interval: $0.044 \leqslant \delta_1 \leqslant 0.047$.

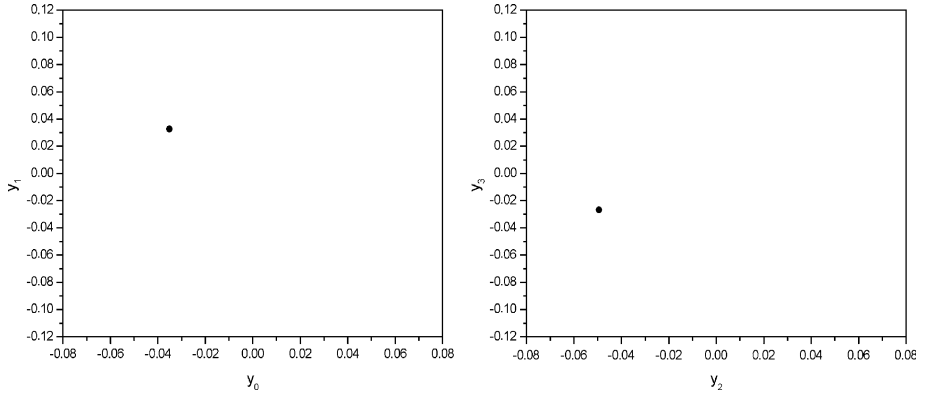

Fig. 15. Periodic response: $\delta_1 = 0.06$, $\delta_2 = 0$ and $(\theta_1, \theta_2, \theta_3) = (1.5, 0.7, 1.5)$.

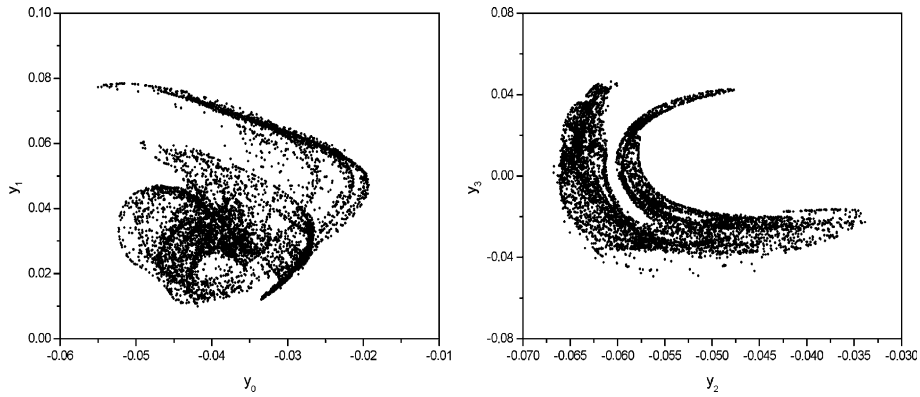

Fig. 16. Chaotic response: $\delta_1 = 0.06$, $\delta_2 = 0$ and $(\theta_1, \theta_2, \theta_3) = (1.5, 1.5, 1.5)$.

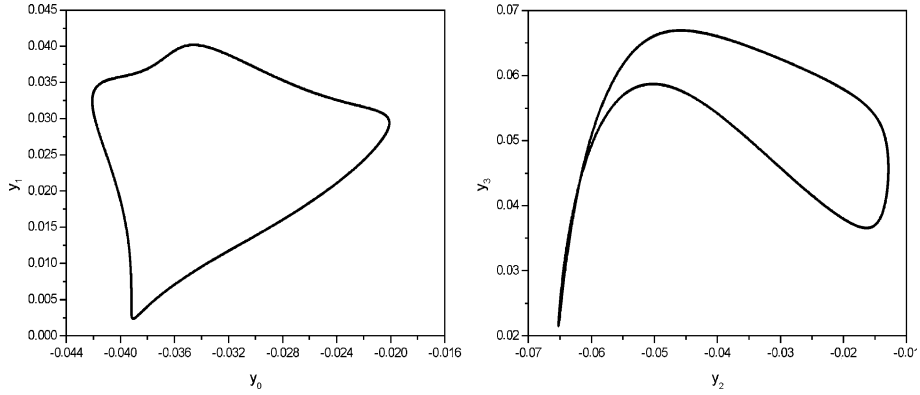

Fig. 17. Quasi-periodic response: $\delta_1 = 0.06$, $\delta_2 = 0$ and $(\theta_1, \theta_2, \theta_3) = (1.5, 3.5, 1.5)$.

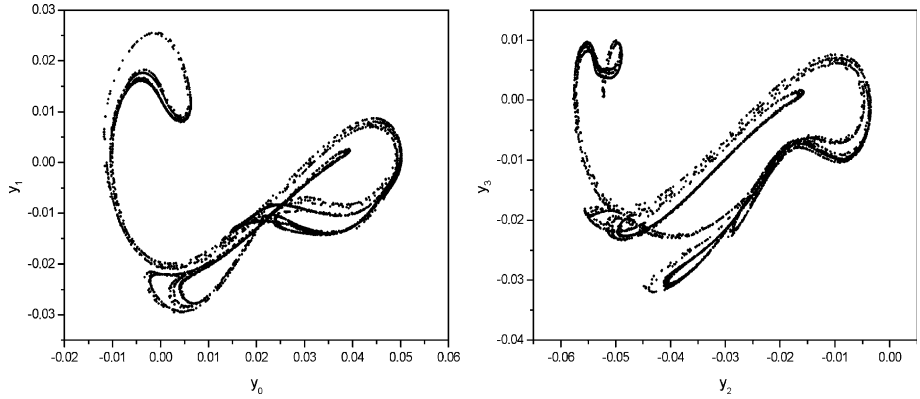

Fig. 18. Chaotic response for $\delta_1 = 0.02$, $\delta_2 = 0$ and $(\theta_1, \theta_2, \theta_3) = (1.5, 0.7, 1.5)$.

By considering the set of parameters $\delta_1 = 0.02$, $\delta_2 = 0$ and $(\theta_1, \theta_2, \theta_3) = (1.5, 0.7, 1.5)$, a strange attractor appears on the phase space, indicating a chaotic motion (Fig. 18). The Lyapunov exponents for this

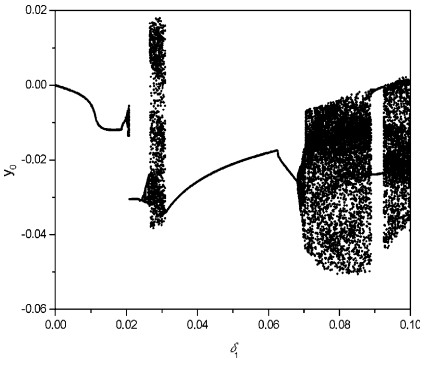

Fig. 19. Bifurcation diagram for $\delta_2 = 0$, $(\theta_1, \theta_2, \theta_3) = (3.5, 0.7, 3.5)$.

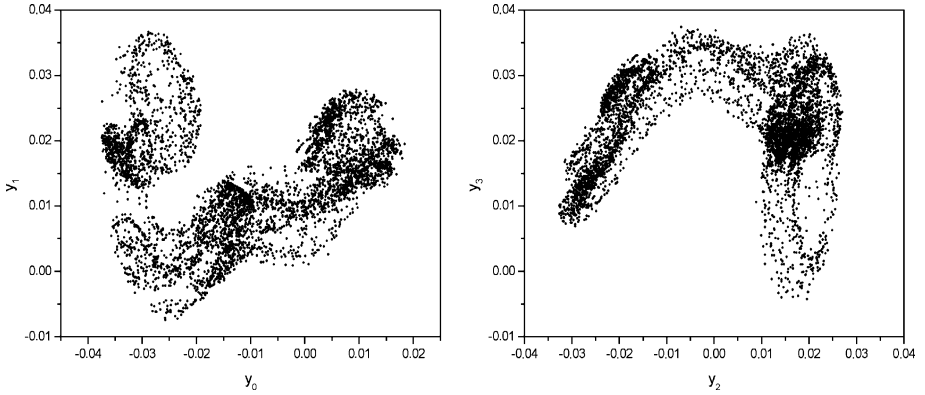

Fig. 20. Chaotic response for $\delta_1 = 0.03$, $\delta_2 = 0$ and $(\theta_1, \theta_2, \theta_3) = (3.5, 0.7, 3.5)$.

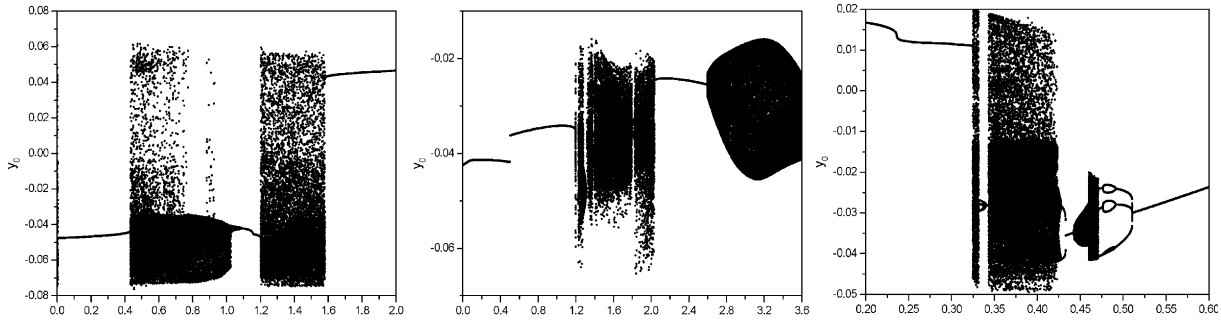

Fig. 21. Bifurcation diagram for θ_2—$\delta_1 = 0.06$, $\delta_2 = 0$: (a) $(\theta_1, \theta_3) = (0.7, 0.7)$; (b) $(\theta_1, \theta_3) = (1.5, 1.5)$; (c) $(\theta_1, \theta_3) = (3.5, 3.5)$.

situation, $\lambda_i = (+0.23, -0.38, -0.44, -0.56)$, assure this behavior. By increasing the temperature connection, either intermediate or high values produce a period-1 response.

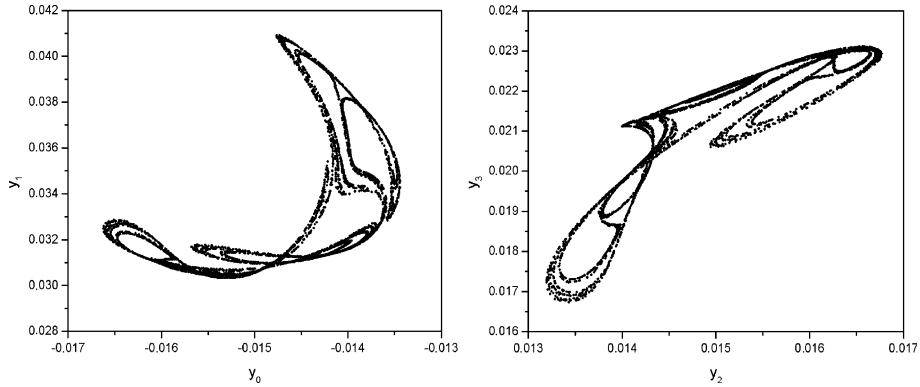

Fig. 22. Strange attractor: $\delta_1 = 0.06$, $\delta_2 = 0$ and $(\theta_1, \theta_2, \theta_3) = (3.5, 0.47, 3.5)$.

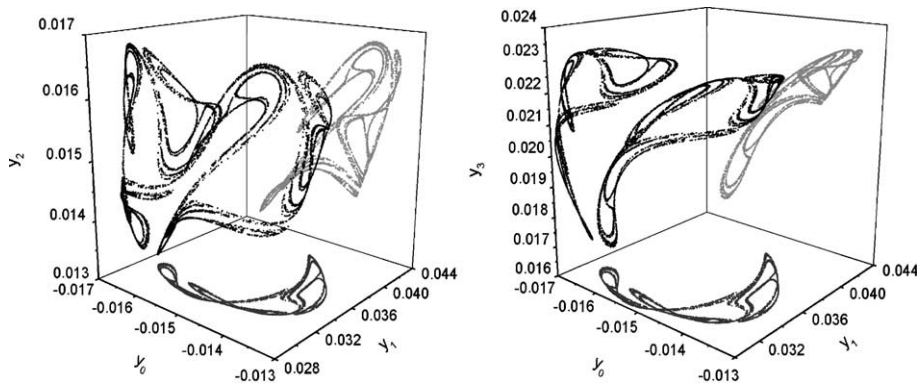

Fig. 23. 3D projections of the strange attractors: $\delta_1 = 0.06$, $\delta_2 = 0$ and $(\theta_1, \theta_2, \theta_3) = (3.5, 0.47, 3.5)$.

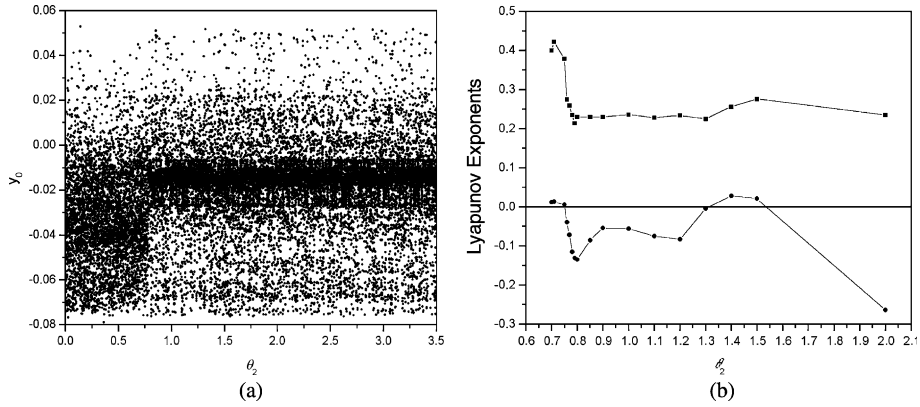

Fig. 24. Chaos–hyperchaos transition—$\delta_1 = 0.06$, $\delta_2 = 0.06$ and $(\theta_1, \theta_3) = (0.7, 0.7)$: (a) bifurcation diagram; (b) Lyapunov exponents.

When all shape memory elements are at a high temperature, i.e., only austenitic phase is stable ($\theta_1 = \theta_2 = \theta_3 = 3.5$), the system presents no bifurcation for the set of parameters considered, leading to

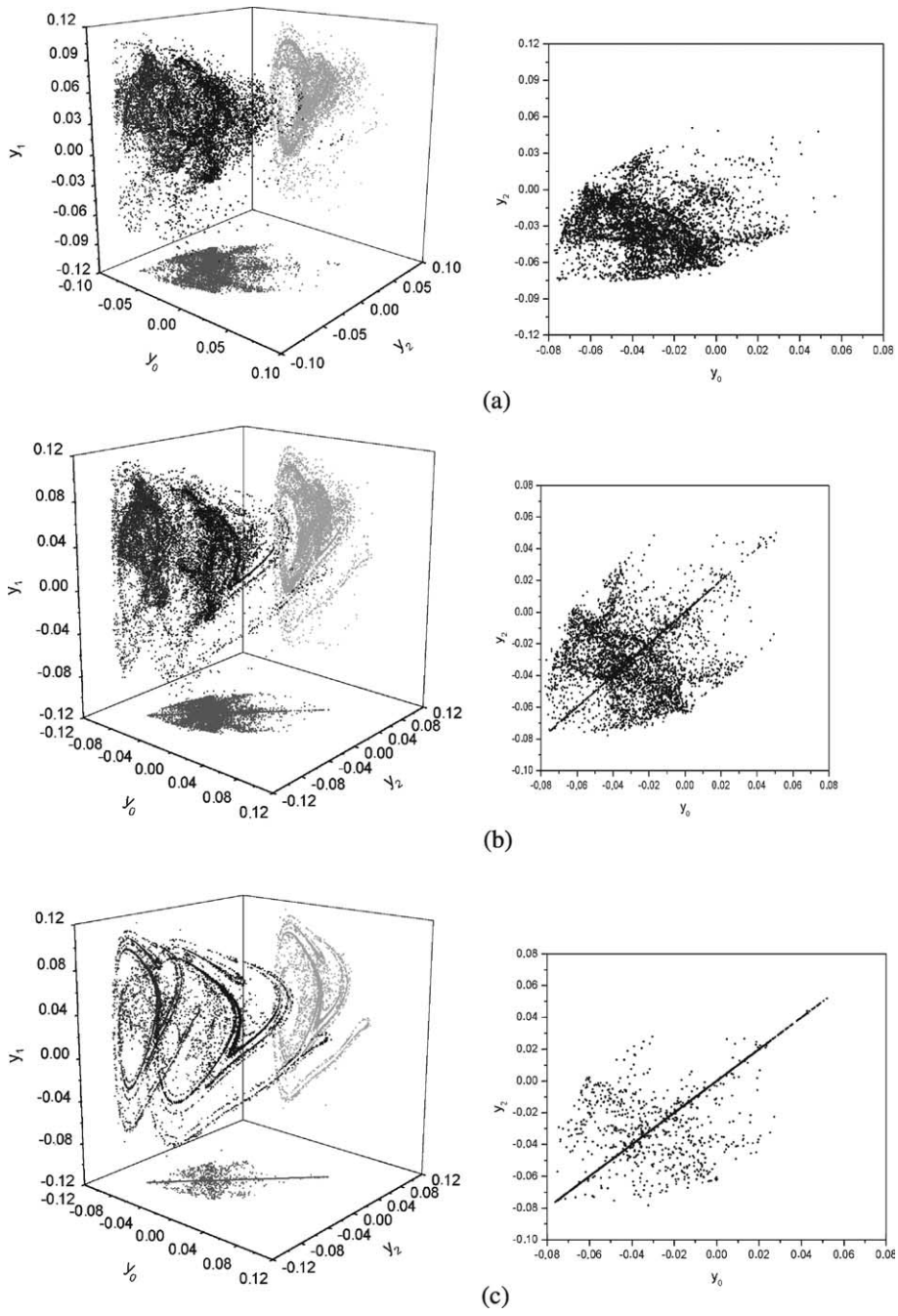

Fig. 25. Chaos–hyperchaos transition, Poincaré sections—$\delta_1 = 0.06$, $\delta_2 = 0.06$, $(\theta_1, \theta_3) = (0.7, 0.7)$: (a) $\theta_2 = 0.7$ – hyperchaos; (b) $\theta_2 = 0.75$ – hyperchaos; (c) $\theta_2 = 0.8$ – chaos; (d) $\theta_2 = 1.2$ – chaos; (e) $\theta_2 = 1.5$ – hyperchaos; (f) $\theta_2 = 2.0$ – chaos.

regular responses. When the temperature connection is $\theta_2 = 1.5$, the system presents no bifurcation, as well. By considering $(\theta_1, \theta_2, \theta_3) = (3.5, 0.7, 3.5)$, however, the bifurcation diagram shows regions associated with

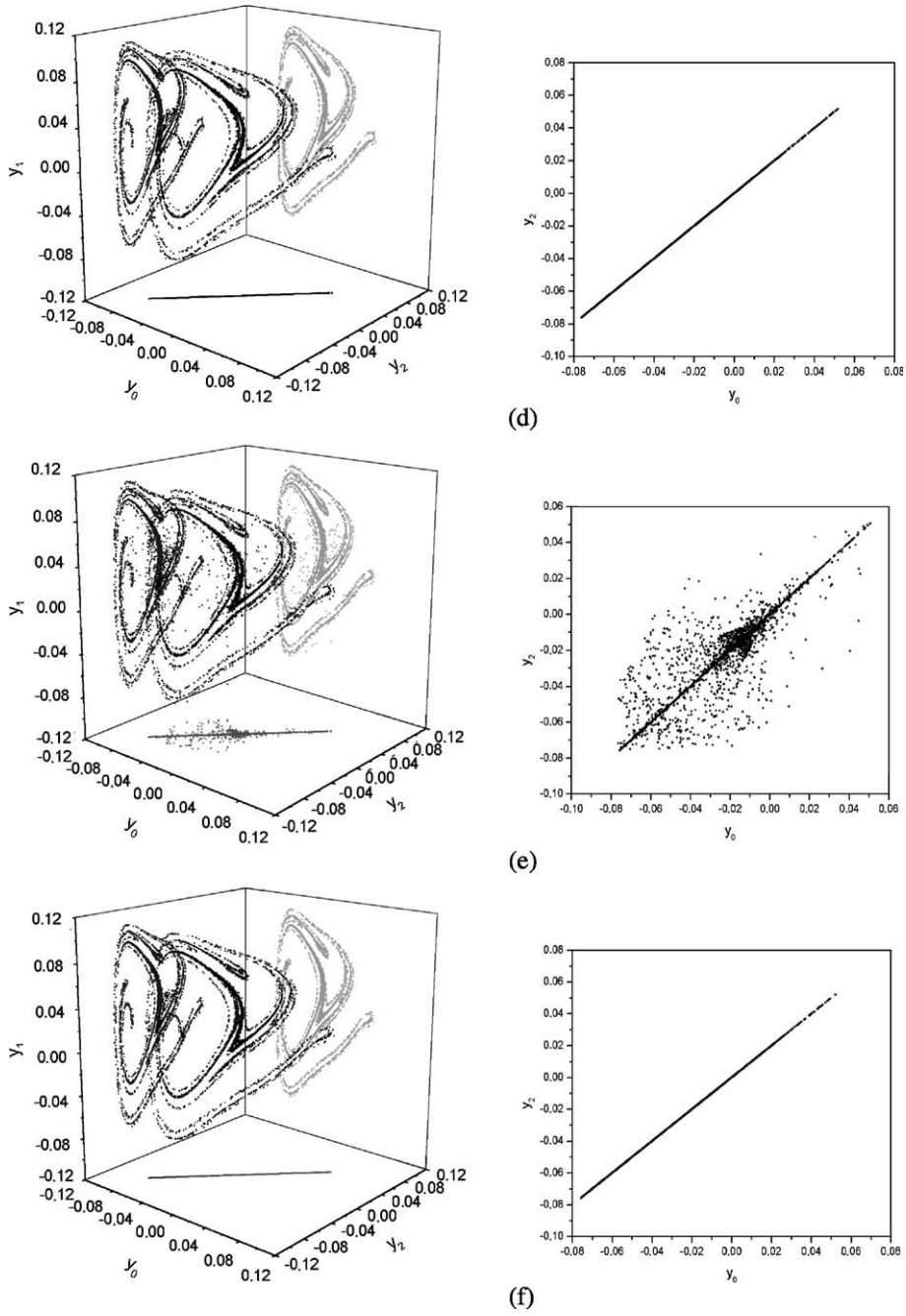

Fig. 25 (*continued*)

chaotic responses (Fig. 19). When $\delta_1 = 0.03$, for example, the system presents a chaotic behavior with $\lambda_i = (+0.36, -0.14, -0.16, -1.21)$ (Fig. 20).

In order to obtain a more detailed analysis of temperature variation on the shape memory system, a bifurcation analysis is performed for $\delta_1 = 0.06$ and $\delta_2 = 0$. Basically a stroboscopical variation of parameter θ_2 is considered. Fig. 21 presents the system response for three different situations: (a) $(\theta_1, \theta_3) = (0.7, 0.7)$, (b) $(\theta_1, \theta_3) = (1.5, 1.5)$ and (c) $(\theta_1, \theta_3) = (3.5, 3.5)$. When $(\theta_1, \theta_3) = (0.7, 0.7)$ (Fig. 21a) the system presents a periodic response on the interval $0 < \theta_2 < 0.4$, becoming chaotic on $0.4 < \theta_2 < 1.0$. Hyperchaos appears when $1.2 < \theta_2 < 1.6$ and, for higher values, the response becomes periodic again. In Fig. 21b, on the other hand, temperatures θ_1 and θ_3 are intermediate. In this case, the interval $1.2 < \theta_2 < 2.0$ presents chaotic behavior. For higher temperatures, such that $\theta_2 > 2.6$, the system presents only quasi-periodic response. Fig. 21c is related to situations in which θ_1 and θ_3 present high temperatures. Temperature changes of the connection show that chaotic responses are observed on the interval $0.325 < \theta_2 < 0.47$.

The preceding analysis allows one to identify chaotic regions. Fig. 22 presents the strange attractor concerning the response for $\delta_1 = 0.06$, $\delta_2 = 0$ and $(\theta_1, \theta_2, \theta_3) = (3.5, 0.47, 3.5)$, while Fig. 23 shows two three-dimensional projections of the corresponding Poincaré sections. The existence of a positive Lyapunov exponent assures this behavior: $\lambda_i = (+0.045, -0.08, -0.329, -0.79)$.

5. Transition chaos → hyperchaos

This section deals with the transition from chaotic to hyperchaotic behavior. Fig. 24 presents the bifurcation diagram and the two major Lyapunov exponents of the system, when the oscillator is subjected to a temperature variation of the connection (parameter θ_2), for the parameters $\delta_1 = 0.06$, $\delta_2 = 0.06$, and $\theta_1 = \theta_3 = 0.7$. Notice that this bifurcation diagram does not allow one to distinguish chaos from hyperchaos.

The evolution of Poincaré sections for $\delta_1 = 0.06$, $\delta_2 = 0.06$, and $(\theta_1, \theta_3) = (0.7, 0.7)$, varying temperature parameter θ_2, is shown in Fig. 25. Two different subspaces are considered in each condition. The first subspace is related to a three-dimensional projection of the phase space, while the second is composed by y_0 and y_2 which correspond to the position of each mass. Fig. 25a shows the response when $\theta_2 = 0.7$, where hyperchaos is observed. Notice that a cloud of points fills the subspace composed by y_0 and y_2. When θ_2 is increased, one can figure out the transition hyperchaos → chaos (Fig. 25b–d). From Fig. 25b, a straight line appears in the y_0–y_2 subspace. Moreover, attractors begin to show a fractal-like pattern. Finally, Fig. 25d shows a chaotic attractor with a well-defined pattern with a fractal-like structure. Besides, y_0–y_2 subspace has a straight line, rather than the cloud of points. Finally, Fig. 25e presents hyperchaos again and Fig. 25f returns to chaos.

6. Conclusions

This article is concerned with the dynamical response of coupled shape memory oscillators. A polynomial constitutive model is assumed to describe the constitutive behavior of the restitution force. Due to its high dimension, the dynamical analysis is performed by splitting the phase space. An analysis of equilibrium points for homogeneous temperatures shows that the system may present 25 equilibrium points for intermediate temperatures, where both martensite and austenite are stables. For lower temperatures, where martensitic phase is stable, the system presents 13 equilibrium points. For higher temperatures, where austenite is stable, the system presents only a fixed point. By considering non-homogeneous temperatures, the number and stability of the equilibrium points varies according to temperatures. Numerical simulations of the free response have shown that the system may present a number of interesting, complex behaviors, including dynamical jumps. The forced response analysis is performed with the aid of Lyapunov exponents. The analysis of temperature characteristics shows how its variation can modify the system

response. Several routes of responses are observed by simply changing the connection temperature. Variations like hyperchaos → chaos → periodic response, and periodic → quasi-periodic → chaos, may occur. These several routes show how intricate and rich is the system behavior. It is also shown that temperature variation may alter either the kind of response or its amplitude. Therefore, it is possible to imagine different applications using SMA as actuators in adaptive structures using temperature as the control variable.

Acknowledgements

The authors acknowledge the support of the Brazilian Agencies CNPq and CAPES.

References

Anokhin, A.P., Lutzenberger, W., Birbaumer, N., 1999. Spatiotemporal organization brain dynamics and intelligence: an EEG study in adolescents. Int. J. Psychophysiol. 33, 259–273.

Awrejcewicz, J., 1991. Bifurcation and Chaos in Coupled Oscillators. World Scientific.

Birman, V., 1997. Review of mechanics of shape memory alloy structures. Appl. Mech. Rev. 50, 629–645.

Boccaletti, S., Grebogi, C., Lai, Y.C., Mancini, H., Maza, D., 2000. The control of chaos: theory and applications. Phys. Rep. 329, 103–197.

Collet, M., Foltête, E., Lexcellent, C., 2001. Analysis of the behavior of a shape memory alloy beam under dynamical loading. Eur. J. Mech. A – Solids 20, 615–630.

Denoyer, K.K., Scott Erwin, R., Rory Ninneman, R., 2000. Advanced smart structures flight experiments for precision spacecraft. Acta Astronautica 47, 389–397.

Duerig, T., Pelton, A., Stöckel, D., 1999. An overview of Nitinol medical applications. Mater. Sci. Engng A 273–275, 149–160.

Falk, F., 1980. Model free-energy, mechanics and thermodynamics of shape memory alloys. Acta Metallurgica 28, 1773–1780.

Gandhi, F., Chapuis, G., 2002. Passive damping augmentation of a vibrating beam using pseudoelastic shape memory alloy. J. Sound Vib. 250 (3), 519–539.

Garner, L.J., Wilson, L.N., Lagoudas, D.C., Rediniotis, O.K., 2001. Development of a shape memory alloy actuated biomimetic vehicle. Smart Mater. Struct. 9 (5), 673–683.

Hodgson, D.E., Wu, M.H., Biermann, R.J., 1992. Shape memory alloys. In: ASM Handbook, vol. 2, pp. 887–902.

Hu, G., Xiao, J., Yang, J., Xie, F., Qu, Z., 1997. Synchronization of saptiotemporal chaos and its applications. Phys. Rev. E 56 (3), 2738–2746.

Lai, Y.-C., Grebogi, C., 1999. Modeling of coupled chaotic oscillators. Phys. Rev. Lett. 82 (24), 4803–4806.

Lagoudas, D.C., Rediniotis, O.K., Khan, M.M., 1999. Applications of shape memory alloys to bioengineering and biomedical technology. In: Proceeding of 4th International Workshop on Mathematical Methods in Scattering Theory and Biomedical Technology, Perdika, Greece.

Machado, L.G., Savi, M.A., 2003. Medical applications of shape memory alloys. Brazilian J. Medical Biological Res. 36 (5).

Pecora, L.M., Carroll, T.L., Johnson, G.A., Mar, D.J., Heagy, J.F., 1997. Fundamentals of synchronization in chaotic systems, concepts, and applications. Chaos 7 (4), 520–543.

Rogers, C.A., 1995. Intelligent materials. Scientific American (September), 122–127.

Saadat, S., Salichs, J., Noori, M., Hou, Z., Davoodi, H., Bar-On, I., Suzuki, Y., Masuda, A., 2002. An overview of vibration and seismic applications of NiTi shape memory alloy. Smart Mater. Struct. 11 (2), 218–229.

Salichs, J., Hou, Z., Noori, M., 2001. Vibration suppression of structures using passive shape memory alloy energy dissipation devices. J. Intelligent Mater. Systems Struct. 12 (10), 671–680.

Savi, M.A., Braga, A.M.B., 1993a. Chaotic vibrations of an oscillator with shape memory. J. Brazilian Soc. Mech. Sci. XV (1), 1–20.

Savi, M.A., Braga, A.M.B., 1993b. Chaotic response of a shape memory oscillator with internal constraints. In: Proceedings of XII the Brazilian Congress of Mechanical Engineering, Brasília, Brasil, pp. 33–36.

Savi, M.A., Pacheco, P.M.L.C., 2002. Chaos and hyperchaos in shape memory systems. Int. J. Bifurcation Chaos 12 (3), 645–657.

Savi, M.A., Pacheco, P.M.L.C., Braga, A.M.B., 2002. Chaos in a shape memory two-bar truss. Int. J. Non-linear Mech. 37 (8), 1387–1395.

Seelecke, S., 2002. Modeling the dynamic behavior of shape memory alloys. Int. J. Non-linear Mech. 37 (8), 1363–1374.

Shibata, H., 1998. Quantitative characterization of spatiotemporal chaos. Physica A 252, 428–449.

Umberger, D.K., Grebogi, C., Ott, E., Afeyan, B., 1989. Spatiotemporal dynamics in a dispersively coupled chain of nonlinear oscillators. Phys. Rev. A 39 (9), 4835–4842.

van Humbeeck, J., 1999. Non-medical applications of shape memory alloys. Mat. Sci. Engng A 273–275, 134–148.

Webb, G., Wilson, L., Lagoudas, D.C., Rediniotis, O., 2000. Adaptive control of shape memory alloy actuators for underwater biomimetic applications. AIAA J. 38 (2), 325–334.

Wolf, A., Swift, J.B., Swinney, H.L., Vastano, J.A., 1985. Determining Lyapunov exponents from a time series. Physica D 16, 285–317.